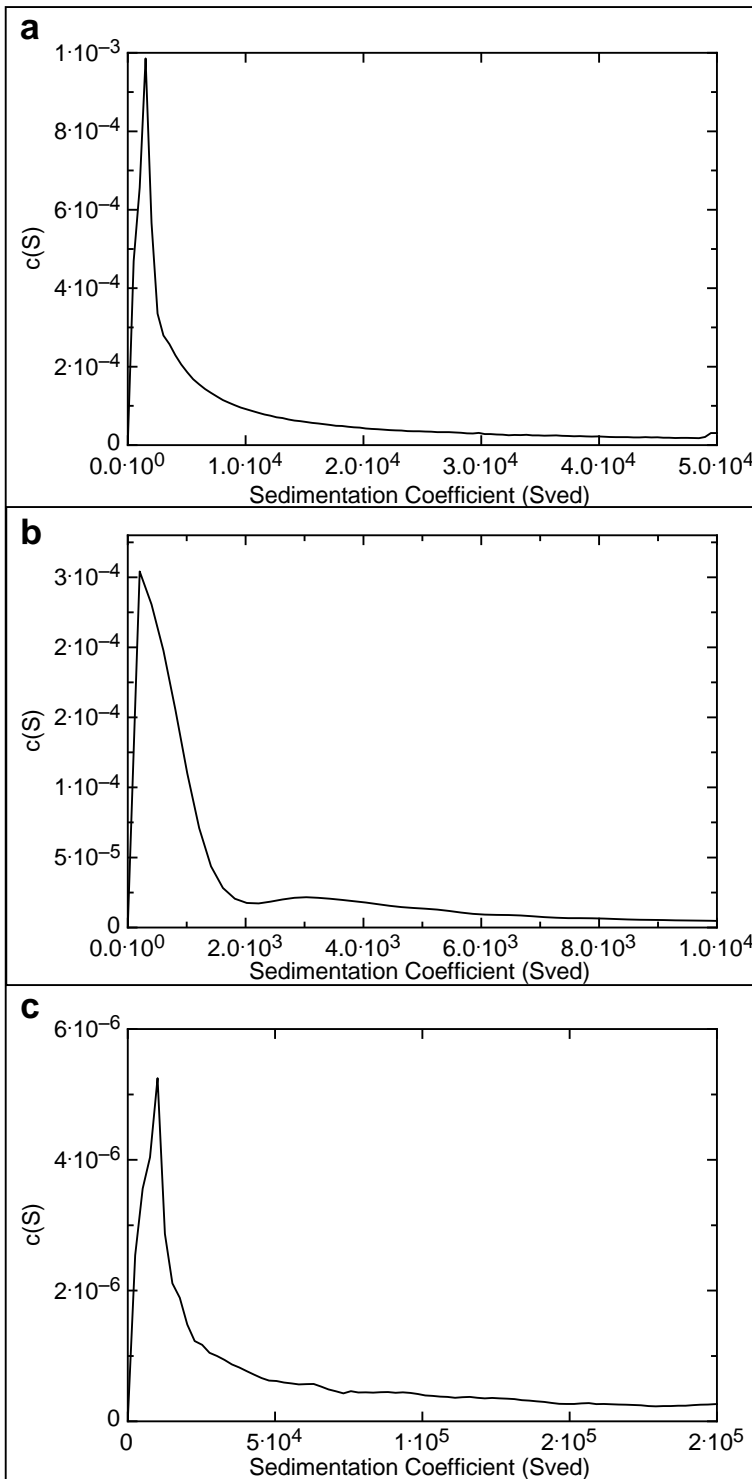
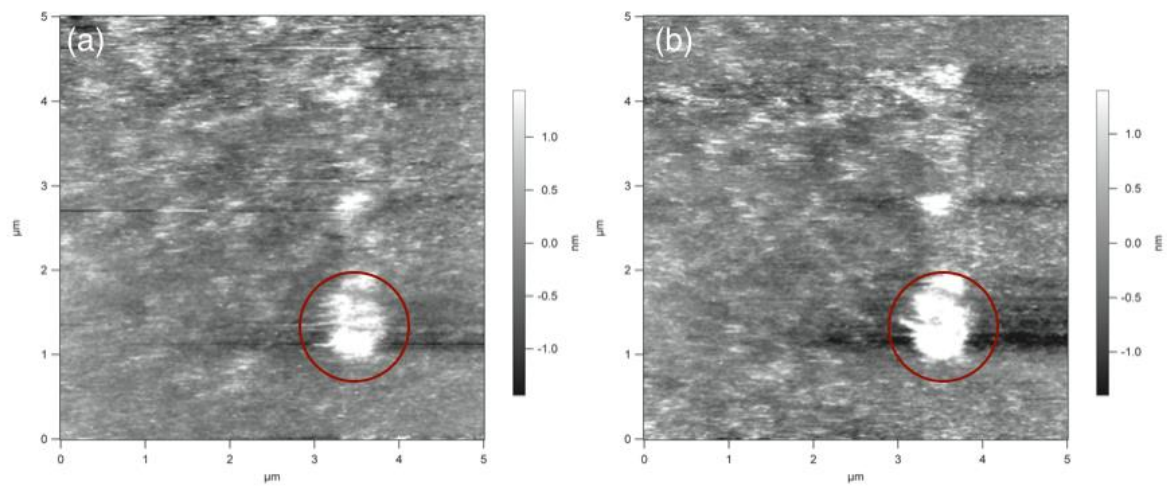


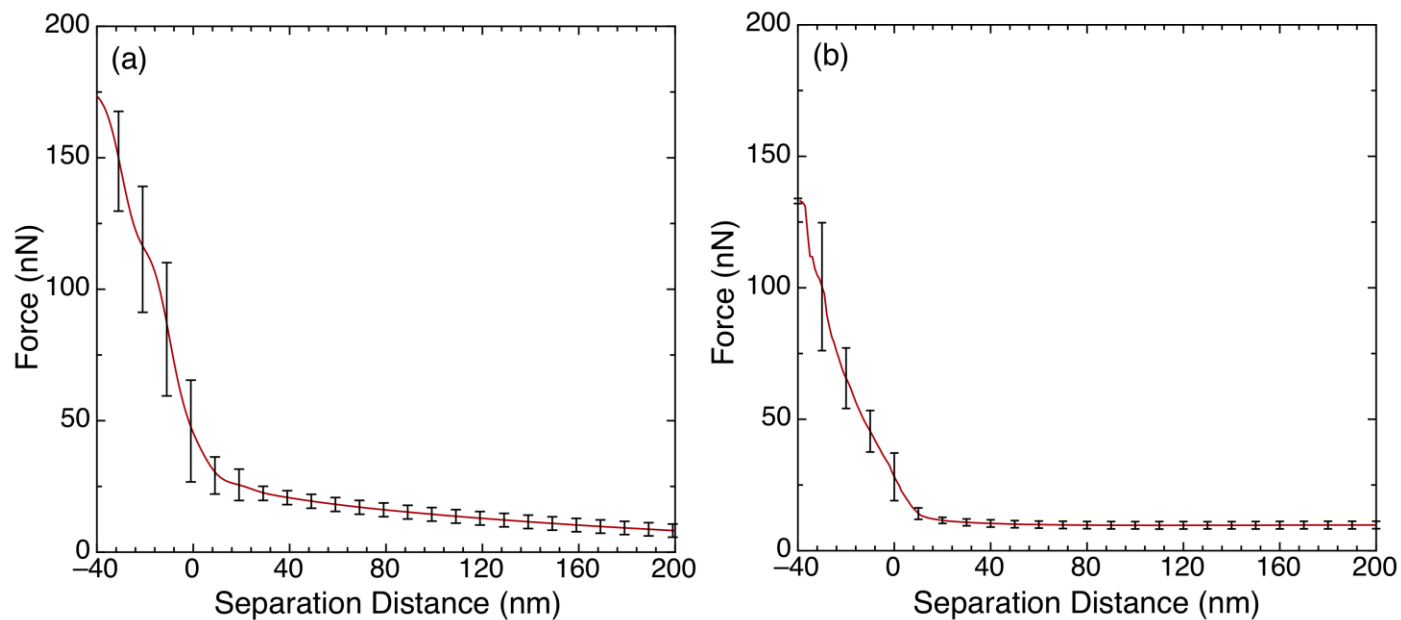
Supplementary Figure 1 | TEM Images of representative ENMs in raw powder form **a**, CeO_2 ($d_{\text{BET}}=5.4$ nm). **b**, CeO_2 ($d_{\text{BET}}=27.9$ nm). **c**, CeO_2 ($d_{\text{BET}}=71.3$ nm). **d**, SiO_2 ($d_{\text{BET}}=18.6$ nm). **e**, Fe_2O_3 ($d_{\text{BET}}=27.6$ nm). **f**, gold nanospheres ($d_{\text{H}}=29$ nm). Scale bars in panels **a-e** = 35 nm, and in panel **f** = 100 nm.



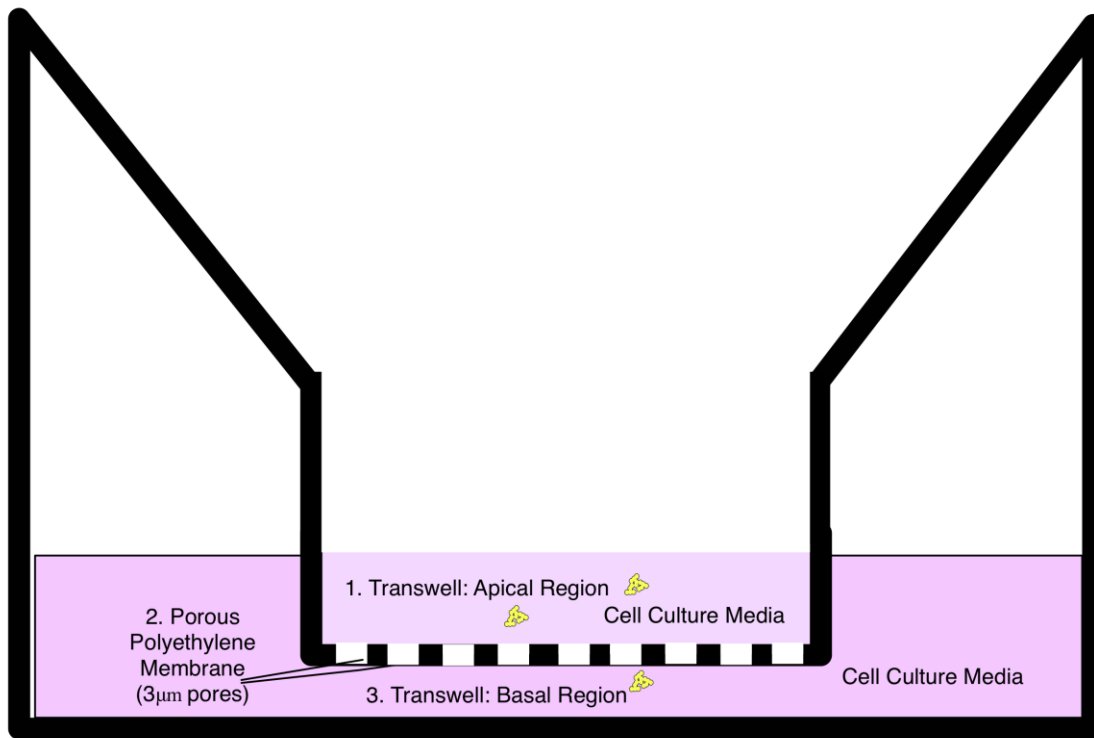
Supplementary Figure 2 | Sedimentation coefficient distributions as determined by analytical ultracentrifugation with interference optics a, CeO₂ ($d_{\text{BET}}=5.4$ nm) dispersed in RPMI/10%FBS. b, SiO₂ ($d_{\text{BET}}=18.6$ nm) dispersed in RPMI/10%FBS. c, Gold nanospheres ($d_{\text{H}}=29$ nm) dispersed in DI H₂O.



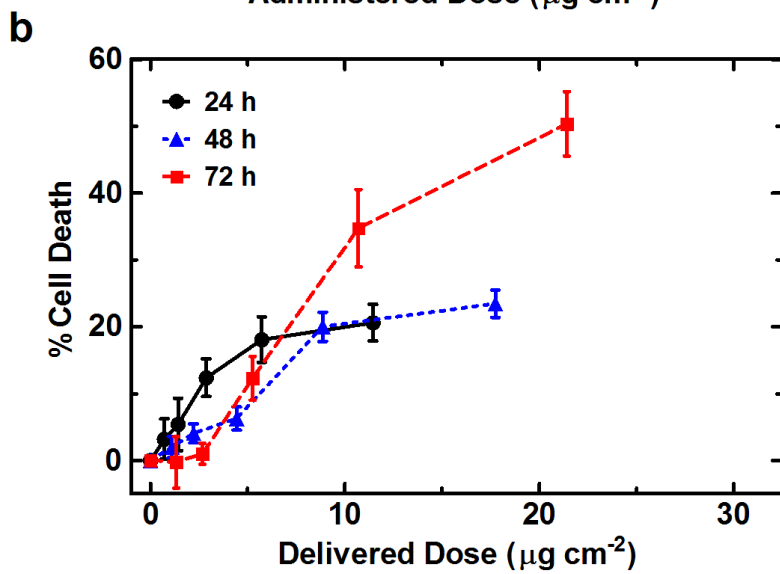
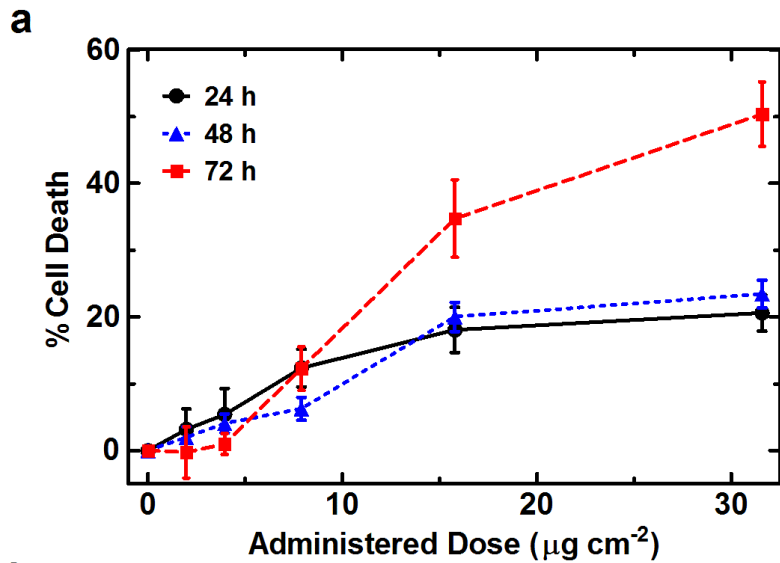
Supplementary Figure 3 | Atomic force microscopy images a, agglomerate prior to application of force. b, agglomerate following application of maximum 150 nN force.



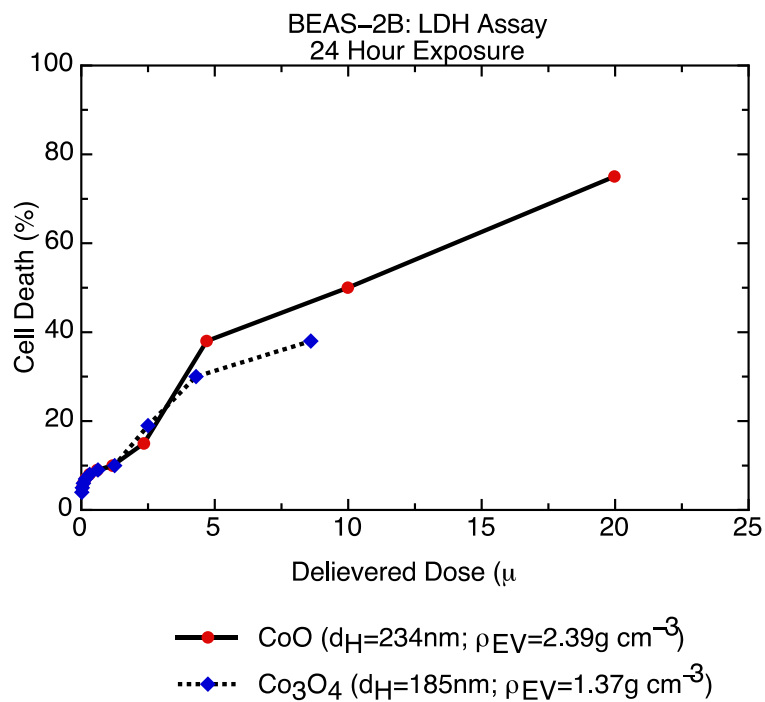
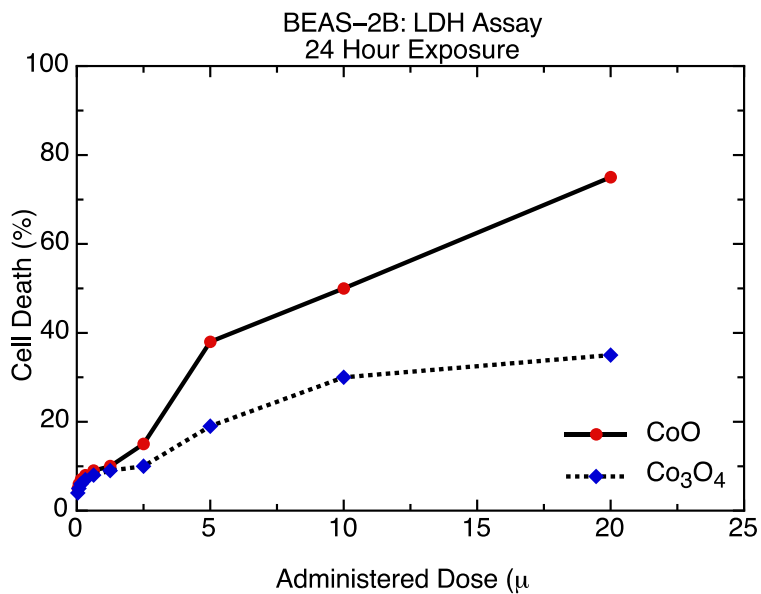
Supplementary Figure 4 | Atomic force microscopy force-displacement curves Applied force plotted as a function of distance between AFM probe tip and substrate for centrifuged and non-centrifuged agglomerates. **a**, average of 20 traces for centrifuged agglomerates. **b**, average of 36 traces for non-centrifuged agglomerates.



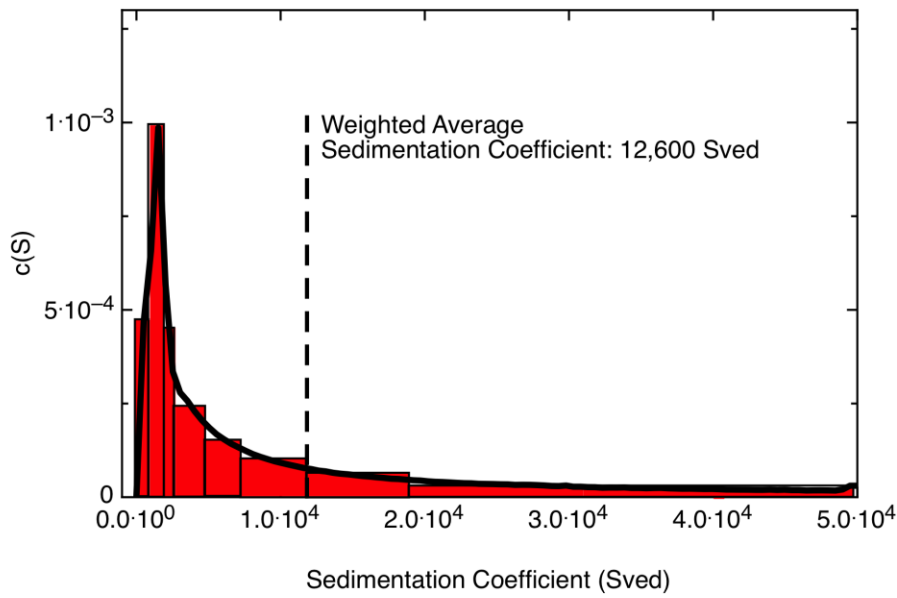
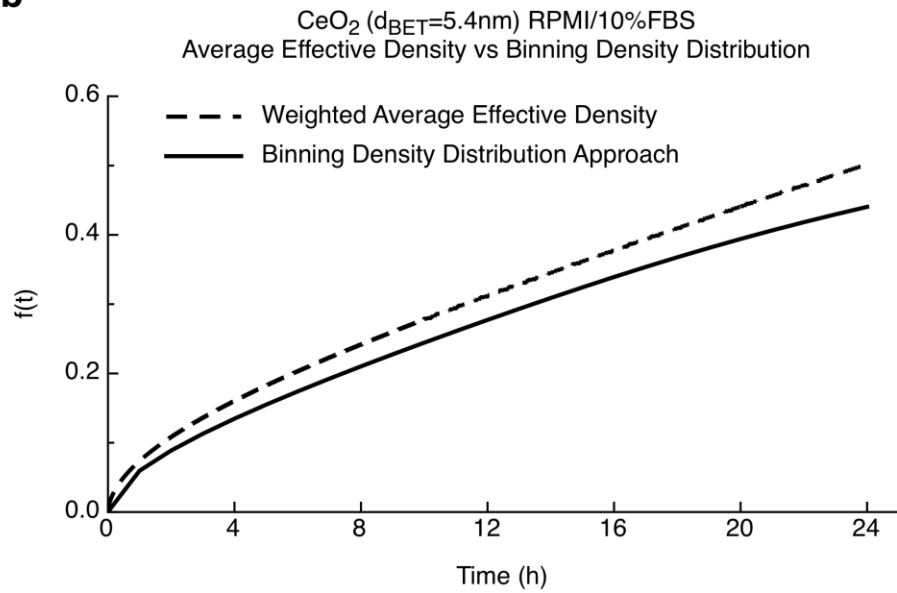
Supplementary Figure 5 | Experimental Setup for dosimetry approach validation experiments



Supplementary Figure 6 | Administered vs. Delivered ENM dose and Cytotoxicity in Calu-3 cells (WST-1 assay) **a**, Cell death in Calu-3 cells as a function of administered dose of CeO_2 ($d_{\text{BET}}=27.9$ nm, $\rho_{\text{EV}}=1.701$ g cm⁻³). **b**, Cell death as a function of mean (time-averaged) delivered dose.



Supplementary Figure 7 | Meta-analysis of Administered vs Delivered Dose and Cytotoxicity in BEAS2-B cells (LDH assay) a. Cell death in BEAS-2B cells as a function of administered dose of CoO and Co₃O₄ (adapted from data presented in Zhang et al 2012). B. Cell death as a function of delivered dose

a**b**

Supplementary Figure 8 | Effect of polydispersity on dosimetry modeling **a**, Binning of sedimentation coefficient distribution for CeO_2 ($d_{\text{BET}}=5.4\text{nm}$) dispersed in RPMI/10%FBS. **b**, Fraction of administered dose deposited, f_D , as a function of time from single weighted average effective density (dashed line), or sum of binned results (solid line).

Supplementary Tables

Supplementary Table 1: Properties of ENM dispersions in RPMI/10%FBS.

Material	d_{BET} (nm)	d_{H} (nm)	PdI	ζ (mV)	σ (mS cm ⁻¹)	pH
VENGES SiO ₂	18.6	135.5 ± 9.53	0.715 ± 0.055	-10.8±1.57	14.1±0.737	7.22±0.074
VENGES Fe ₂ O ₃	27.6	380 ± 3.60	0.151 ± 0.070	-12.2±0.929	12.2±0.751	7.74±0.086
VENGES CeO ₂	5.4	179 ± 3.76	0.294 ± 0.022	-14.3±0.751	10.4±0.1	8.16±0.062
VENGES CeO ₂	13.3	181±29.8	0.120±0.095	-12.0 ± 0.329	11.9 ± 0.0883	8.19 ± 0.073
VENGES CeO ₂	71.3	131 ± 5.17	0.171 ± 0.021	-9.77±0.497	11±0.152	7.95±0.05
EVONIK SiO ₂	14	147 ± 3.04	0.031 ± 0.022	-12.2 ± 0.25	11.3±0.17	8.43±0.081
EVONIK TiO ₂	21	457 ± 20.9	0.177 ± 0	-10.9±0.55	10.5±0.42	8.45±0.11
Sigma CuO	58.0	310 ± 7.57	0.269 ± 0.024	-9.43±0.497	11.6±0.493	7.85±0.08
Alfa Aesar ZnO	63	307±96.5	0.303±0.122	-8.94±1.22	12.5±1.82	7.74± 0.11
Au Nanospheres	NA*	42.2±24.7	0.403±0.207	-9.29±2.0	12.0±1.14	7.70 ± 0.13

d_{H} : hydrodynamic diameter, PdI: polydispersity index, ζ : zeta potential, σ : specific conductance

Supplementary Table 2: Optimization of centrifugation speed.

Speed (× g)	ρ_{EV} (g cm ⁻³)	%M _{ENMsn}	ρ'_{EV} (g cm ⁻³)
1000	1.342 ± 0.006	3.35 ± 0.037	1.534 ± 0.009
2000	1.303 ± 0.004	1.68 ± 0.076	1.474 ± 0.007
3000	1.321 ± 0.003	0.763 ± 0.012	1.502 ± 0.005

CeO₂ ($d_{BET}=5.4\text{nm}$, material density (ρ_{ENM}) = 7.215 g/cm³) dispersed at 100µg/ml in RPMI/10%FBS, and centrifuged for 1 hour.

ρ_{EV} : effective density by volumetric centrifugation. %M_{ENMsn} : percent mass remaining in supernatant, ρ'_{EV} : effective density corrected for ENM remaining in supernatant.

Supplementary Table 3: Optimization of ENM concentration.

Concentration ($\mu\text{g cm}^{-3}$)	ρ_{EV} (g cm^{-3})
50	1.365 ± 0.000
100	1.474 ± 0.007
250	1.465 ± 0.004

CeO_2 ($d_{\text{BET}}=5.4$ nm, material density ($\rho_{\text{ENM}} = 7.215$ g cm^{-3}) dispersed in RPMI/10%FBS, and centrifuged at $2000 \times g$ for 1 hour. ρ_{EV} : effective density by volumetric centrifugation.

Supplementary Table 4: Comparison of effective densities in different media formulations.

Media	ρ_{media} (g cm⁻³)	ρ_{EV} (g cm⁻³)
RPMI/10%FBS	1.0084	1.474 ± 0.007
RPMI	1.0072	1.363 ± 0.003
F12K/10%FBS	1.0084	1.374 ± 0.012
F12K	1.007	1.300 ± 0.018

CeO₂ ($d_{\text{BET}}=5.4\text{nm}$, material density ($\rho_{\text{ENM}} = 7.215 \text{ g cm}^{-3}$) dispersed at 100 $\mu\text{g/ml}$ in either RPMI/10%FBS, RPMI alone, F12K/10%FBS, or F12K alone, and centrifuged at $2000 \times g$ for 1 hour: ρ_{media} : media density, ρ_{EV} : effective density by volumetric centrifugation.

Supplementary Notes

Supplementary Note 1: Particle transport

Particle transport in static uniform solutions at constant temperature is primarily driven by diffusion and sedimentation. For the purpose of modeling particle transport in an *in vitro* system, diffusion and sedimentation velocities can be estimated based on the following equations adapted from (1).

According to Fick's first law a substance flows from a region of higher concentration to a region of lower concentration at a flux proportional to the magnitude of the concentration gradient:

$$J = -D \frac{\partial \varphi}{\partial x} \quad (1)$$

where φ is the concentration (mol m^{-3}), x is the position (m), and D is the diffusion coefficient ($\text{m}^2 \text{s}^{-1}$), which is defined by the Stokes-Einstein equation as:

$$D = \frac{k_B T}{3\pi\eta d} \quad (2)$$

where k_B is the Boltzmann constant ($\text{kg m}^2 \text{s}^{-2} \text{K}^{-1}$), T is the absolute temperature (K), η is the media dynamic viscosity ($\text{kg m}^{-1} \text{s}^{-1}$), and d is the particle diameter (m) in suspension.

A particle sediments at a rate, v_s , determined by the balance of forces acting upon the particle: the acceleration force (e.g. gravitational or centrifugal), F_a , the counter buoyant force, F_b , caused by displacement of medium by the particle, and the frictional, or drag force, F_d .

$$F_a + F_b + F_d = 0 \quad (3)$$

The gravitational force is the product of the acceleration due to gravity, g (m s^{-2}) and the mass of the particle, m_p (kg):

$$F_a = gm_p \quad (4)$$

The buoyant force opposing the acceleration force is the product of the acceleration and the mass of the displaced media, m_{media} (kg):

$$F_b = -gm_{media} \quad (5)$$

The frictional or drag force is defined by Stokes' law as

$$F_d = -fv_s, \quad (6)$$

where f is the frictional coefficient, which for a spherical particle is given by

$$f = 3\pi\eta d. \quad (7)$$

Substituting supplementary equations (4-7) into supplementary equation (3), replacing mass with the products of volume and density, and rearranging yields

$$v_s = \frac{g\left(\frac{1}{6}\pi d^3\right)(\rho_p - \rho_{media})}{3\pi\eta d}, \quad (8)$$

where ρ_p is the particle density (kg m^{-3}), ρ_{media} is the media density (kg m^{-3}). Simplifying supplementary equation 8 yields

$$v_s = \frac{g(\rho_p - \rho_{media})d^2}{18\eta}. \quad (9)$$

The sedimentation coefficient of a particle, s , is defined as the ratio of a particle's terminal velocity to the acceleration applied to it, e.g.:

$$s = \frac{v_s}{g} \quad (10)$$

The sedimentation coefficient of a protein or small particle can be measured by analytical ultracentrifugation (AUC), wherein the gravitational acceleration in supplementary equation 10 is replaced by the centrifugal field:

$$s = \frac{v_s}{\omega^2 r}, \quad (11)$$

where ω is the angular velocity (rad s^{-1}) and r is the distance of the particle from the center of revolution.

Supplementary Note 2: Effective density estimation using the Sterling equation

In the Sterling model, the effective density of an ENM in suspension, ρ_{ES} , is calculated from the primary particle density, ρ_{p} , and media density, ρ_{media} , as:

$$\rho_{\text{ES}} = (1 - \varepsilon_a) \rho_{\text{p}} + \varepsilon_a \rho_{\text{media}}, \quad (12)$$

where ε_a is the agglomerate porosity, which in turn is estimated from the single ENM particle diameter as determined by the Brunauer Emmet Teller method, d_{BET} , the agglomerate hydrodynamic diameter, d_{H} , and a theoretical fractal dimension, DF , as:

$$\varepsilon_a = 1 - \left(\frac{d_{\text{H}}}{d_{\text{BET}}} \right)^{DF-3}. \quad (13)$$

Supplementary Note 3: estimating effective ENM density by volumetric centrifugation

The effective density of an ENM agglomerate in a liquid suspension, ρ_{EV} , is defined as

$$\rho_{\text{EV}} = \frac{M_{\text{agg}}}{V_{\text{agg}}}, \quad (14)$$

where M_{agg} and V_{agg} are the ENM agglomerate mass and volume, respectively. Since agglomerates are composed of ENM particles and media trapped between primary ENM particles (intra-agglomerate media), the agglomerate mass can be expressed as

$$M_{\text{agg}} = M_{\text{media}} + M_{\text{ENM}}, \quad (15)$$

where M_{media} and M_{ENM} are the masses of intra-agglomerate media and ENM, respectively (see Figure 1). Expressing density in terms of mass and volume, and substituting into supplementary equation 12 yields

$$\rho_{\text{EV}} = \frac{(\rho_{\text{media}} V_{\text{media}}) + (\rho_{\text{ENM}} V_{\text{ENM}})}{V_{\text{agg}}}, \quad (16)$$

where ρ_{media} and ρ_{ENM} are the densities (g cm^{-3}) of the media and ENM, respectively, and V_{media} and V_{ENM} are the volumes of the media and ENM, respectively.

Following centrifugation the pellet collected in the volumetric capillary of a PCV tube consists of stacked ENM agglomerates and inter-agglomerate media interspersed between agglomerates (which is distinct from intra-agglomerate media trapped within agglomerates) (Figure 1). From the measured volume of the pellet, V_{pellet} (cm^3), V_{agg} , can be estimated as

$$V_{\text{agg}} = V_{\text{pellet}} \times SF, \quad (17)$$

where the inter-agglomerate media is accommodated by a stacking factor, SF (volume/volume, unitless), which denotes the fractional contribution of the ENM agglomerates to the pellet.

The intra-agglomerate media volume, V_{media} can then be calculated as

$$V_{\text{media}} = V_{\text{agg}} - V_{\text{ENM}}. \quad (18)$$

The volume of ENM in the pellet, V_{ENM} , can be calculated from the ENM density and the mass of ENM dissolved or remaining in the supernatant, M_{ENMsol} can be calculated as follows

$$V_{\text{ENM}} = \frac{M_{\text{ENM}} - M_{\text{ENMsol}}}{\rho_{\text{ENM}}}. \quad (19)$$

M_{ENMsol} can be directly measured by inductively coupled plasma mass spectrometry (ICP-MS) analysis of supernatants as described in methods. Substituting the expressions for V_{agg} , V_{media} , and V_{ENM} from supplementary equations (15), (16) and (17), respectively, into supplementary equation (14), the effective agglomerate density, ρ_{EV} , can be expressed as

$$\rho_{\text{EV}} = \frac{\rho_{\text{media}} \left(V_{\text{pellet}} SF - \frac{M_{\text{ENM}} - M_{\text{ENMsol}}}{\rho_{\text{ENM}}} \right) + \rho_{\text{ENM}} \left(\frac{M_{\text{ENM}} - M_{\text{ENMsol}}}{\rho_{\text{ENM}}} \right)}{V_{\text{pellet}} SF}, \quad (20)$$

which can be simplified and rewritten as

$$\rho_{\text{EV}} = \rho_{\text{media}} + \left[\left(\frac{M_{\text{ENM}} - M_{\text{ENMsol}}}{V_{\text{pellet}} SF} \right) \left(1 - \frac{\rho_{\text{media}}}{\rho_{\text{ENM}}} \right) \right]. \quad (21)$$

Finally for insoluble materials, if we assume the contribution of M_{ENMsol} to be negligible (which we have verified from ICP-MS analysis of supernatants), supplementary equation (19) can be simplified to yield

$$\rho_{EV} = \rho_{\text{media}} + \left[\left(\frac{M_{\text{ENM}}}{V_{\text{pellet}} SF} \right) \left(1 - \frac{\rho_{\text{media}}}{\rho_{\text{ENM}}} \right) \right]. \quad (22)$$

Supplementary Discussion

Forces and agglomerate compression by atomic force microscopy

Supplementary Figure 3 shows images of centrifuged aggregates before and after a maximum force of 150 nN was applied with the AFM tip. There is no significant difference between the images. The observed alteration before and after the application of the force is due to artifacts of imaging in liquid. More importantly, the average curve of applied force clearly demonstrates that the tip experienced a constant repulsion, increasing with the distance between AFM tip and substrate (Supplementary Figure 4). Similar results were obtained for aggregates deposited without centrifugation.

Had the agglomerates been physically compressed by the applied force, a distinct dip in the force-distance curve would have been observed². In both cases, aggregates were stable for forces exceeding 100 nN, which is more than six orders of magnitude greater than the forces experienced during centrifugation by either individual aggregates (0.063 fN) or by whole agglomerates (90 fN). In terms of pressure, agglomerates withstood 2.98 GPa applied by AFM, which is again more than six orders of magnitude greater than pressures experienced during centrifugation by aggregates (5.06 Pa) or whole agglomerates (0.183 kPa).

These data confirm that the forces exerted on agglomerates during volumetric centrifugation are considerably smaller than those that would be required to alter their structure, and suggest that agglomerates do not collapse and their structures remain uncompromised during volumetric centrifugation.

Effect of polydispersity on modeled transport

The fraction of administered dose delivered as a function of time based on mean density vs. binned density is shown in Supplementary Figure 8b. The two methods estimate very similar deposition kinetics for this material, with only a 6% difference in the estimated delivered dose after 24 hours (44% estimated by the binning approach vs. 50% by the weighted average approach). These results clearly demonstrate that a weighted average value for effective density (equivalent to the effective density value estimated using our volumetric centrifugation approach) closely approximates the particle deposition kinetics for a polydisperse suspension, and can be used to accurately estimate dosimetry for in vitro nanotoxicology studies.

Supplementary Methods

Calculation of forces on agglomerates during centrifugation

The potentially deforming forces exerted on suspended nano-agglomerates during volumetric centrifugation can be considered in two different ways: I. Forces act on individual primary particles (aggregates) results in their collapsing individually into the agglomerate; and II. forces on the agglomerate as a whole results in closer packing of primary particles (aggregates) within the agglomerate.

Case I: Each primary particle or aggregate collapses individually into the agglomerate. In this case the force F (N, or kg m s^{-2}) exerted on each primary particle is:

$$F = m_{\text{ENM}} \times RCF \times g = \frac{4}{3} \pi r_{\text{ENM}}^3 \times \rho_{\text{ENM}} \times RCF \times g \quad (23)$$

where r_{ENM} is the primary particle radius (m), RCF is the relative centrifugal force, g is the gravitational acceleration (9.8 m s^{-2}), and ρ_{ENM} is the material density (kg cm^{-3}). For CeO_2 with $r_{\text{ENM}} = 4.75 \times 10^{-9} \text{ m}$ and $\rho = 7215 \text{ kg m}^{-3}$, at $RCF = 2000$, equation 23 yields a force of 0.063 fN (or $6.3 \times 10^{-17} \text{ N}$). One could argue that the relevant force is the pressure exerted per unit area of particle surface, which would be a much larger value since the particle dimensions are very small. Thus, assuming for the particle under consideration that the area of contact has an average diameter of 4 nm, the resulting pressure P is 5.06 N m^{-2} (Pa) or about or $5 \times 10^{-5} \text{ atm}$.

Case II: Primary particles or aggregates are packed such that the relevant force is that exerted on the entire agglomerate. This force can be calculated as:

$$F = m_{agg} \times RCF \times g = \frac{4}{3} \pi r_H^3 \times \rho_E \times RCF \times g \quad (24)$$

where m_{agg} is the mass of an agglomerate, r_H is the hydrodynamic radius (m), and ρ_E is the effective density of the agglomerate in suspension (kg m^{-3}). For CeO_2 with $r_H = 9.0 \times 10^{-8}$ m and $\rho_H = 1532 \text{ kg m}^{-3}$, at $RCF = 2000$, equation 24 yields a force of For CeO_2 $r_H = 9.0 \times 10^{-8}$ m, $\rho_E = 1532 \text{ kg m}^{-3}$, the resulting force is 90 fN (or 9.0×10^{-14} N) and the pressure (assuming F is applied over the cross sectional area of the agglomerate) is 7.83 kPa, or about 0.08 atm.

Atomic force microscopy of agglomerates

Suspensions of CeO_2 particles ($d_{\text{BET}}=9$ nm) in RPMI/FBS were prepared as described in methods in the main body of the text. A <111> silicon wafer (Ted Pella, Redding, CA), which had been previously cleaned with 0.1 N HCl in a sonication bath for 20 min. and then serially washed with ethanol and water, was placed in a 2.0 ml centrifuge tube, oriented parallel to the bottom of the tube, and 1.0 ml of the ENM suspension was added drop-wise to the tube. The tube was centrifuged at $2000 \times g$ for one hour in order to force deposition of particles onto the wafer. The suspension liquid was then removed with a pipette (and reserved) leaving a small layer of liquid to avoid artifacts from fast drying of particles. The wafer was then removed from the tube and placed on a kim-wipes to dry the bottom surface. The wafer was then fixed on slide glass with epoxy, and once the epoxy was solidified 100 μl of the reserved suspension liquid was added to cover the wafer. AFM probes used were AC240T (Asylum Research, Santa Barbara, CA). The spring constant was measured according to the protocol suggested from the manufacturer using a freshly prepared silicon wafer ($k=1.18 \text{ nN nm}^{-1}$). The imaging scan rate was 1 Hz and the scanned area $5 \mu\text{m} \times 5 \mu\text{m}$ with 256 scan lines. Images were flattened with Asylum Software (range of 100 nm and threshold of 100 pm) for the mask and 1st order image flattening. The prepared sample was placed on the stage of the Asylum MFP-3D with the addition of a small amount of reserved suspension liquid to facilitate engagement of the tip holder with the substrate, as suggested by the manufacturer.

The substrate was imaged and once an aggregate was identified the tip was guided on top of the aggregate and used to apply forces up to 150 nN. Both trace and retrace curves were obtained. In a second approach, the aggregates were left to deposit on the substrate without any centrifugation. A mica slide was fixed on glass with epoxy and cleaved, and was used to measure the tip constant (1.83 nN nm^{-1}). A small amount of the particle suspension was added to the mica surface and the tip holder to facilitate engagement of the tip and substrate. After 1 h forces were measured in various locations of the substrate.

Cytotoxicity Experiments

Human lung epithelial cell (Calu-3, ATCC, Manassas, VA) were cultured in Minimum Essential Medium Eagle (EMEM) media supplemented with L-Glutamine, Penicillin-Streptomycin and 2% Fetal Bovine Serum.

Cytotoxicity was analyzed by the 4-[3-(4-iodophenyl)-2-(4-nitrophenyl)-2H-5-tetrazolio]-1,3-benzene disulfonate (WST-1) assay (Roche Diagnostic, Mannheim, Germany) according to the manufacturer's instructions. Briefly, cells (3×10^3 cells well⁻¹) were cultured in 96-well plates and treated with CeO₂ ($d_{\text{BET}} = 27.9 \text{ nm}$) dispersed in cell culture media at $0\text{-}100 \mu\text{g cm}^{-3}$, and 1% Triton X-100 in saline as a positive control (Triton X-100, Sigma Aldrich, St Louis, MO, USA). Following exposures of either 24, 48, or 72 hours cells were washed with PBS and incubated for 4 hours with 100 μl of WST-1 dye. Absorbance was measured at 450 nm using a Spectra max 250 plate reader (Molecular Devices, Sunnyvale, CA, USA). Sample absorbance (A_{450}) values were normalized with negative control (particle free media) and positive control (Triton X) absorbance values, to calculate percent cell viability as follows:

$$viability(\%) = \frac{A_{450}(\text{sample}) - A_{450}(\text{neg.control})}{A_{450}(\text{pos.control}) - A_{450}(\text{neg.control})} \quad (25)$$

Modeling transport with accounting for polydispersity

The sedimentation profile for CeO₂ ($d_{\text{BET}}=5.4 \text{ nm}$) suspended in RPMI/10%FBS was divided into 10 bins, each corresponding to 10% of the total population of particles within the distribution, and a median sedimentation

coefficient was calculated for each bin (Supplementary Figure 7a). The ISDD model was used to model transport separately for each bin (inputting DLS-derived hydrodynamic diameter and effective density estimated from the median sedimentation coefficient for the bin). All other parameters were as described in methods for ISDD modeling. The combined fraction of administered dose deposited as a fraction of time was calculated as the weighted sum of the fractions deposited for the individual bins.

Supplementary References

1. van Holde, K. E., Johnson, W.C., Ho, P.S. *Principles of Physical Biochemistry* Ch. 5 (Prentice Hall, Upper Saddle River, NJ, 1998)
2. Rabinovich, Y., Pandey S., Shah, D.O., Moudgil, B.M. Effect of the chain-length compatibility of surfactants and mechanical properties of mixed micelles on surfaces. *Langmuir* **22**, 6858–6862 (2006)